ELSEVIER

Journal of Alloys and Compounds 311 (2000) 101–108

Journal of ALLOYS AND COMPOUNDS

www.elsevier.com/locate/jallcom

Antiferro- to ferromagnetic transition in $HfFe_6Ge_6$-type solid solution $YMn_6Ge_{6-x}Ga_x$ $(0.25 \leqslant x \leqslant 2.00)$

G. Venturini*

Laboratoire de Chimie du Solide Minéral, Université Henri Poincaré-Nancy I, associé au CNRS (UMR 7555), B.P. 239, 54506 Vandoeuvre les Nancy Cedex, France

Received 3 March 2000; accepted 14 March 2000

Abstract

The $HfFe_6Ge_6$-type $YMn_6Ge_{6-x}Ga_x$ solid solution $(0.25 \leqslant x \leqslant 2.00)$ has been studied by magnetization measurements. The low Ga content compounds $(x \leqslant 0.75)$ behave as antiferromagnetic $(475 \geqslant T_N \geqslant 404$ K). The Ga-rich compounds $(1.25 \leqslant x \leqslant 2.00)$ are ferromagnetic $(352 \geqslant T_c \geqslant 310$ K). The intermediate compounds display metamagnetic behaviour with rather weak threshold fields $(H_t < 0.5$ T). The moments deduced from the maximum magnetization values in the ferromagnetic state are close to 1.8 μ_B per Mn atom. The evolution of the magnetic properties with Ge substitution is discussed.

Keywords: Rare earth compounds; Transition metal compounds; Magnetically ordered materials; Magnetization; Phase transition

1. Introduction

The magnetic properties of the hexagonal $HfFe_6Ge_6$-type RMn_6X_6 compounds (R = rare earth metal, X = Ge, Sn) have been studied extensively [1–4]. The compounds of diamagnetic R elements (R = Sc, Y, Lu) display antiferromagnetic or helimagnetic structures characterized by ferromagnetic (001) planes and various interplane couplings [5–8]. Ferromagnetic behaviour has been evidenced in the solid solution $(Mg,Ca)Mn_6Sn_6$ involving alkaline earth metals [9]. On the contrary, the IVA compounds (Zr, Hf) display antiferromagnetic structures or helimagnetic arrangements with propagating vector values indicating a strengthening of the antiferromagnetic interactions [8,10]. Therefore, the evolution of the magnetic properties of MMn_6X_6 as a function of M (M = IIA, IIA, IVA metals, X = Ge, Sn) indicates that the interplane couplings are strongly related to the M valency and it is also suggested that change of the X valency may have significant effects on the magnetic properties of the Mn sublattice.

Recent studies on $Y(Ga,Ge)_{\approx 2}$ solid solutions have shown the effect of germanium substitution on the crystallographic properties of these phases [11]. Therefore, it was decided to examine the magnetic behaviour of $HfFe_6Ge_6$-type solid solutions involving gallium and germanium.

2. Experimental

The various compounds used in this study were prepared by alloying stoichiometric amounts of YMn_6Ge_6 and YMn_6Ga_6 samples previously prepared in an induction furnace. The mixtures were finely ground, compacted into pellets, sealed in silica tubes under argon and annealed at 1100 K for 1 week. After this first thermal treatment, the samples were ground, compacted again and annealed at 1023 K for 10 days. The purity of the samples was checked by powder X-ray analysis (Guinier Co Kα). The corresponding patterns display the lines typical of the $HfFe_6Ge_6$ structure. Some weak and diffuse lines belonging to an unknown compound are also observed.

Cell parameters were refined by a least squares procedure from Guinier patterns recorded with high-purity silicon ($a = 5.43082$ Å) as internal standard.

The magnetic properties were studied using a MANICS magneto-susceptometer in fields up to 1.5 T and in the temperature range 10–600 K.

3. Results

3.1. Crystallographic data

The whole $YMn_6Ge_{6-x}Ga_x$ series $(0.25 \leqslant x \leqslant 2.00)$ crystallizes in the $HfFe_6Ge_6$-type structure. The cell

E-mail address: venturin@lcsm.u-nancy.fr (G. Venturini).

0925-8388/00/$ – see front matter
PII: S0925-8388(00)00816-1

Table 1
Summary of the crystallographic and magnetic properties of $YMn_6Ge_{6-x}Ga_x$ compounds ($0.25 \leq x < 2.00$)

x	a (Å)	c (Å)	V (Å^3)	c/a	T_N (K)	T_c (K)	H_t (300 K) (T)	H_t (10 K) (T)	M_{max} (10 K) (μ_B/f.u.)
0.25	5.232(2)	8.159(5)	193.4(3)	1.5594	475	–	>1.6	>1.6	1.20
0.50	5.233(2)	8.168(3)	193.7(2)	1.5609	453	–	>1.6	>1.6	1.97
0.75	5.231(3)	8.173(5)	193.7(4)	1.5624	414	–	>1.6	>1.6	4.70
1.00	5.230(2)	8.181(3)	193.8(2)	1.5642	404	–	>1.6	0.28	5.80
1.05	5.229(2)	8.192(3)	194.0(2)	1.5666	364	–	0.41	0.20	9.71
1.10	5.229(2)	8.201(4)	194.2(3)	1.5683	347	–	0.08	0	10.56
1.15	5.232(2)	8.207(4)	194.6(2)	1.5686	347	–	0	0	10.60
1.25	5.228(2)	8.207(4)	194.8(3)	1.5698	–	352	0	0	10.66
1.50	5.229(2)	8.226(4)	194.8(2)	1.5731	–	340	0	0	10.45
1.75	5.228(2)	8.244(5)	195.2(3)	1.5769	–	328	0	0	9.98
2.00	5.230(3)	8.261(5)	195.7(4)	1.5795	–	310	0	0	9.68

parameters and volumes of the studied compounds are shown in Table 1. The a parameter does not vary significantly, while a rather large increase of the c parameter with gallium content is observed.

3.2. Isotherm curves

Figs. 1 and 2 display the magnetization curves measured at 300 and 10 K. At room temperature and in the 0–1.5 T

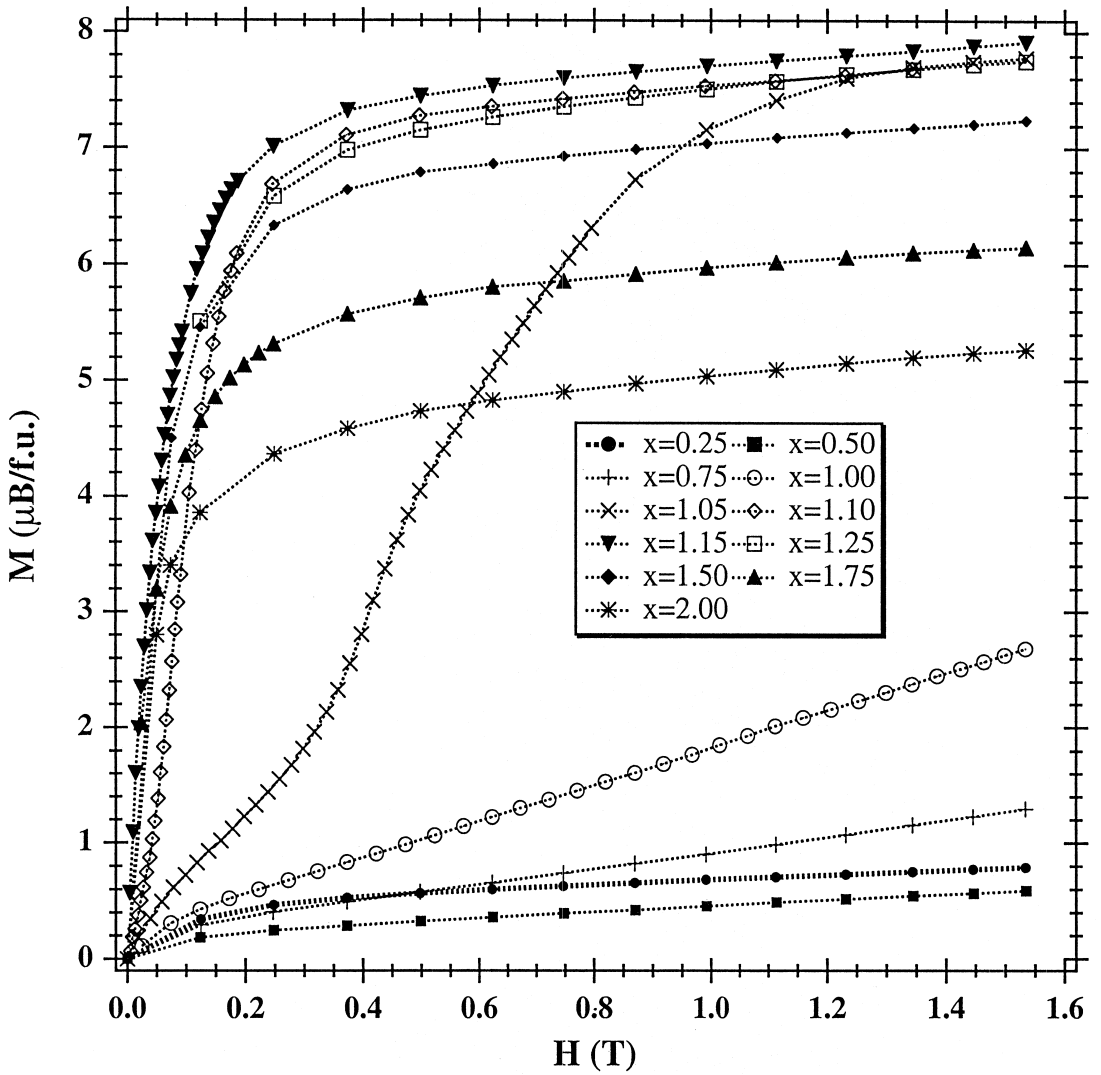

Fig. 1. Magnetization vs. applied field at 300 K for $YMn_6Ge_{6-x}Ga_x$ ($0.25 \leq x \leq 2.00$).

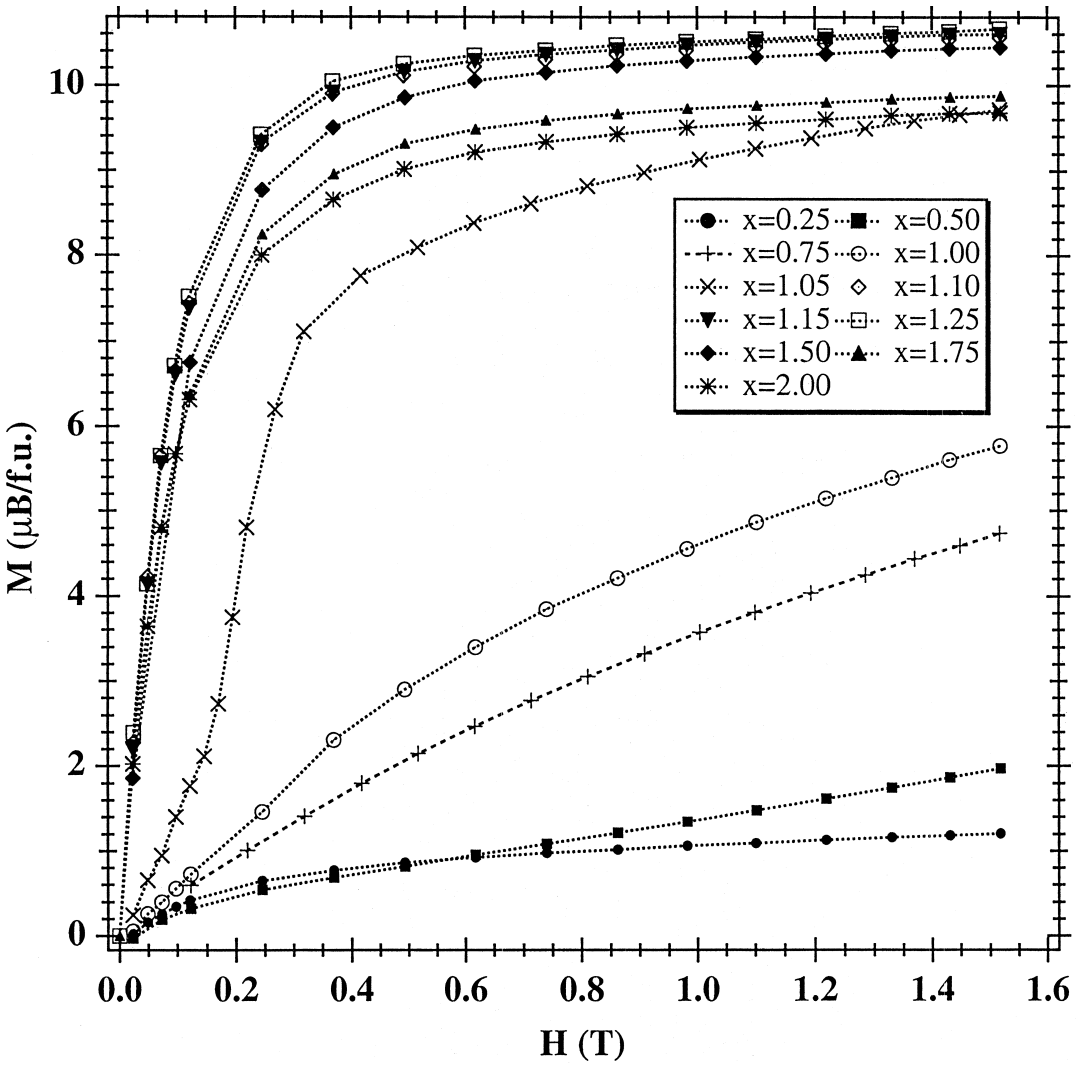

Fig. 2. Magnetization vs. applied field at 10 K for $YMn_6Ge_{6-x}Ga_x$ ($0.25 \leq x \leq 2.00$).

field range investigated, the magnetizations of $YMn_6Ge_{6-x}Ga_x$ samples ($x \leq 1.0$) vary linearly. Weak and variable spontaneous magnetizations are also measured. They might be attributed to the presence of different amounts of a ferromagnetic impurity and related to the extra lines observed in the X-ray patterns. The magnetization curves of the $YMn_6Ge_{6-x}Ga_x$ samples ($1.15 \leq x \leq 2.0$) display ferromagnetic behaviour. The maximum values of the magnetization are large ($\approx 8\ \mu_B$/mol). The intermediate compounds ($1.05 \leq x \leq 1.10$) exhibit metamagnetic behaviour. The corresponding threshold fields decrease from 0.41 to 0.08 T when the gallium content increases ($x = 1.05$–1.1). Hence, they are considerably reduced with respect to the values measured in YMn_6Ge_6 (>10 T) [12].

Similar features are observed in the low-temperature measurements. The saturation magnetizations of the ferromagnetic samples are still larger than those measured at room temperature, giving rise to a ferromagnetic moment of about 1.8 μ_B per manganese atom, slightly weaker than the value measured in YMn_6Ge_6 by neutron diffraction (1.95 μ_B/Mn) [5]. The spontaneous magnetizations measured in the antiferromagnetic compounds are slightly larger than the corresponding values measured at room temperature, but remain weak. This is compatible with the presence of ferromagnetic impurities.

The $YMn_6Ge_{4.9}Ga_{1.1}$ compound, metamagnetic at 300 K ($H_t = 0.08$ T), displays ferromagnetic behaviour at low temperature. On the contrary, the magnetization curve of the $YMn_6Ge_5Ga_1$ compound, linear at 300 K, displays a slight curvature at 10 K around 0.3 T. These features indicate that the threshold fields vary with the temperature. The thermal variation of the metamagnetic behaviour was checked for the $YMn_6Ge_{4.95}Ga_{1.05}$ compound (Fig. 3). It clearly shows the decrease of the threshold fields with temperature. This suggests that the strength of the antiferromagnetic interactions decreases with temperature.

3.3. Thermomagnetic curves

The thermal variations of the magnetization are plotted in Figs. 4 and 5 and the ordering temperatures are gathered

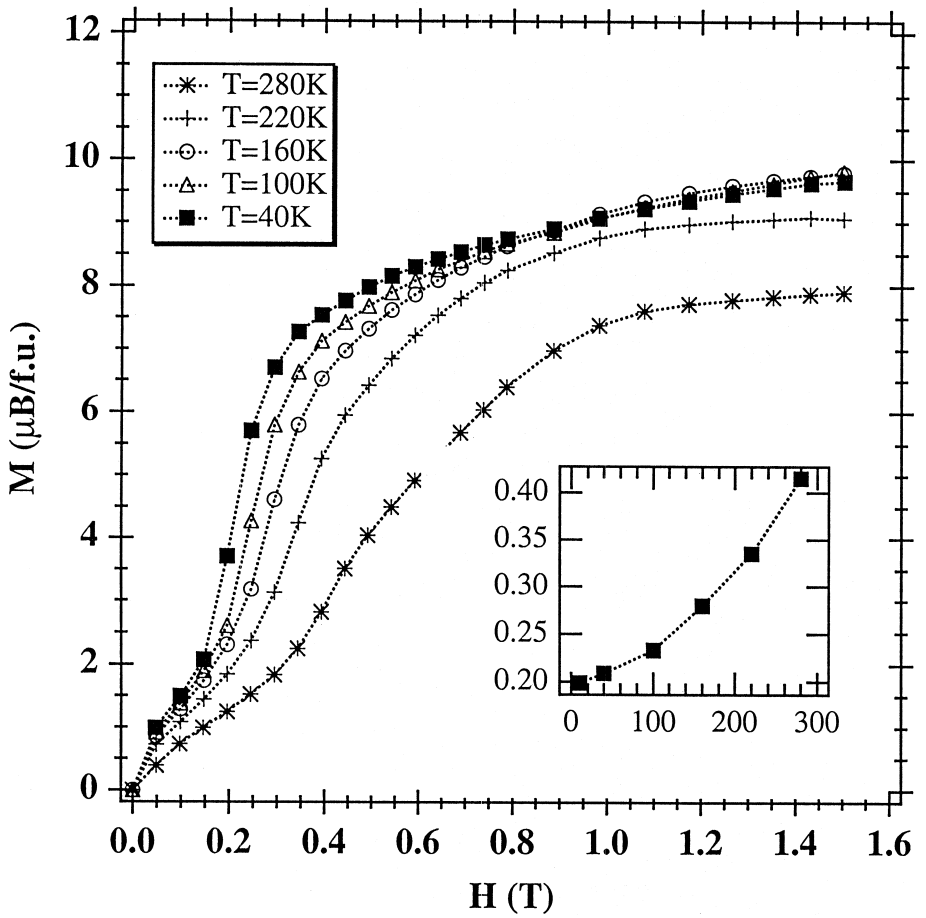

Fig. 3. Magnetization vs. applied field at various temperatures for $YMn_6Ge_{4.95}Ga_{1.05}$ compounds (insert shows the thermal variation of the threshold field).

in Table 1. The thermomagnetic curves of the $YMn_6Ge_{6-x}Ga_x$ compounds ($0 \leq x \leq 1.15$) display more or less pronounced Néel points ranging from 475 K for $YMn_6Ge_{5.75}Ga_{0.25}$ to 347 K for $YMn_6Ge_{4.85}Ga_{1.15}$. The magnetic transitions observed in the $YMn_6Ge_{5.75}Ga_{0.25}$ thermomagnetic curve around 370 K should be attributed to the Curie point of the ferromagnetic impurity. The large increase of the magnetization below 260 K for $YMn_6Ge_{5.25}Ga_{0.75}$ and below 120 K for $YMn_6Ge_{5.50}Ga_{0.50}$ should be attributed to intrinsic magnetic transitions. The isotherm curves recorded at 80 and 150 K for $YMn_6Ge_{5.50}Ga_{0.50}$ do not evidence a significant increase of the spontaneous magnetization below the transition temperature (inset of Fig. 4), thus excluding a ferromagnetic canting of the structure.

Fig. 5 shows the drastic changes in the magnetic behaviour of $YMn_6Ge_{6-x}Ga_x$ compounds around $x = 1.10$. The $YMn_6Ge_5Ga_1$ and $YMn_6Ge_{4.95}Ga_{1.05}$ compounds display weak Néel points at 404 and 364 K and their magnetization remains weak down to 10 K. The $YMn_6Ge_{4.9}Ga_{1.1}$ and $YMn_6Ge_{4.85}Ga_{1.15}$ compounds are characterized by more pronounced Néel points and large increases of the magnetization at lower temperature. The shape of the $YMn_6Ge_{4.9}Ga_{1.1}$ curve should be related to the metamagnetic behaviour of this compound and to the variation of the corresponding threshold field. This compound is metamagnetic at room temperature with $H_t = 0.08$ T and ferromagnetic at low temperature. In the applied field used (0.025 T), it behaves as an antiferromagnetic around 300 K and becomes ferromagnetic at lower temperature. The behaviour of the $YMn_6Ge_{4.85}Ga_{1.15}$ compound indicates a still weaker threshold field.

The compounds characterized by larger gallium contents ($1.25 \leq x \leq 2$) are characterized by pronounced Curie points. The ordering temperatures decrease slightly with gallium content from 352 K for $YMn_6Ge_{4.75}Ga_{1.25}$ to 310 K for $YMn_6Ge_4Ga_2$. The variation of the ordering temperatures is weaker for the ferromagnetic compounds ($\Delta T_c/\Delta x \approx 56$ K) than for the antiferromagnetic compounds ($\Delta T_N/\Delta x \approx 142$ K).

4. Discussion

Study of the solid solution $YMn_6Ge_{6-x}Ga_x$ ($0 \leq x \leq 2$) provides interesting results concerning the complicated magnetic behaviour of the manganese atoms in $HfFe_6Ge_6$-type compounds. The evolution with the gallium content

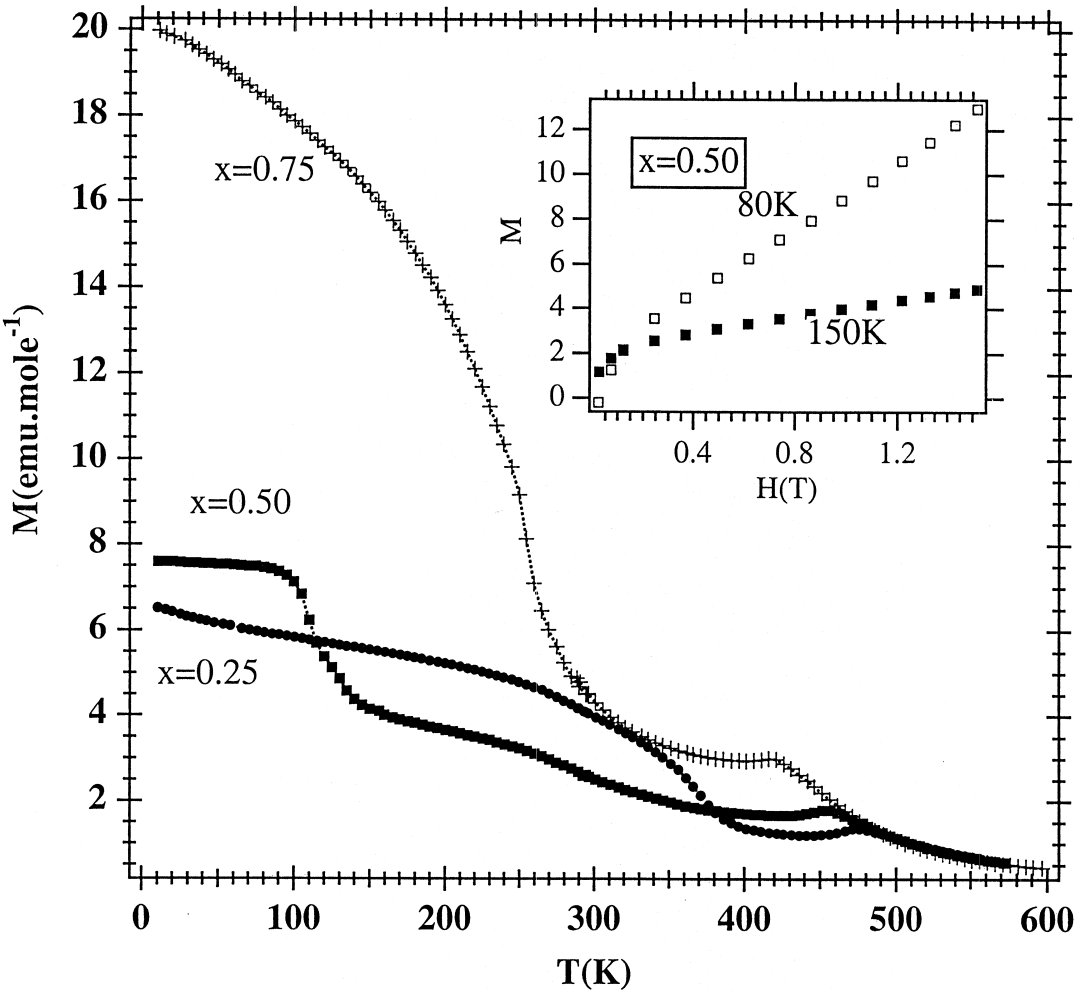

Fig. 4. Temperature dependence of the magnetization of $YMn_6Ge_{6-x}Ga_x$ compounds ($0.25 \leq x \leq 0.75$) in an applied field of 0.8 T (insert shows the field dependence of the $YMn_6Ge_{5.5}Ga_{0.5}$ magnetization below and above the low-temperature magnetic transition).

may be interpreted considering the actual knowledge of the properties of the ternary compounds.

Amongst the numerous $HfFe_6Ge_6$-type MMn_6X_6 (M = rare earth or alkaline earth metal, IIIA or IVA transition element; X = Ge, Sn) germanides and stannides, most of the non-magnetic M compounds display antiferromagnetic behaviour. It may be interpreted on the basis of the interactions scheme depicted in Fig. 6. The occurrence of ferromagnetic (001) Mn planes indicates a positive J_0 intraplane interaction. The parallel alignment of the moments belonging to the Mn–X–Mn sheet also strongly suggests a positive J_1 interplane interaction. The determination of the sign of the J_2 and J_3 interactions is more ambiguous, but the occurrence of helimagnetic structures with a non-parallel alignment of the moments belonging to the Mn–(X,R)–Mn sheet strongly suggests competition between opposite J_2 and J_3 interactions.

Until now there were two ways to obtain a parallel alignment of the Mn moments belonging to the Mn–(X,R)–Mn sheet: the replacement of the diamagnetic rare earth metal by an alkaline earth metal as observed in the $(Mg,Ca)Mn_6Sn_6$ solid solution [9] or the replacement of the diamagnetic R metal by a paramagnetic one [13–16]. In the latter case, the Mn moments are forced to be parallel through the strong Mn–R coupling acting in the Mn–(X,R)–Mn sheet. It is worth noting that this parallel alignment is easily obtained amongst the ternary stannides [13,14], but the helimagnetic structures prevail amongst the ternary germanides [15–20]. This suggests that the antiferromagnetic interactions are stronger in the latter case. Moreover, the helimagnetic structures of the paramagnetic R germanides are characterized by non-parallel alignment of the Mn moments belonging to the Mn–X–Mn sheet [15–20]. This indicates that, when the angles of the Mn moments belonging to the Mn–(X,R)–Mn sheet are small (due to the strong Mn–R interactions), antiferromagnetic interactions tend to open the angle of the moments belonging to the Mn–X–Mn sheet. This suggests that the J_1 interaction also competes with the J_3 interaction. As the J_1 interaction is presumably positive, it may be inferred that the J_3 interaction is negative and, in turn, that the J_2 interaction is positive. According to this view,

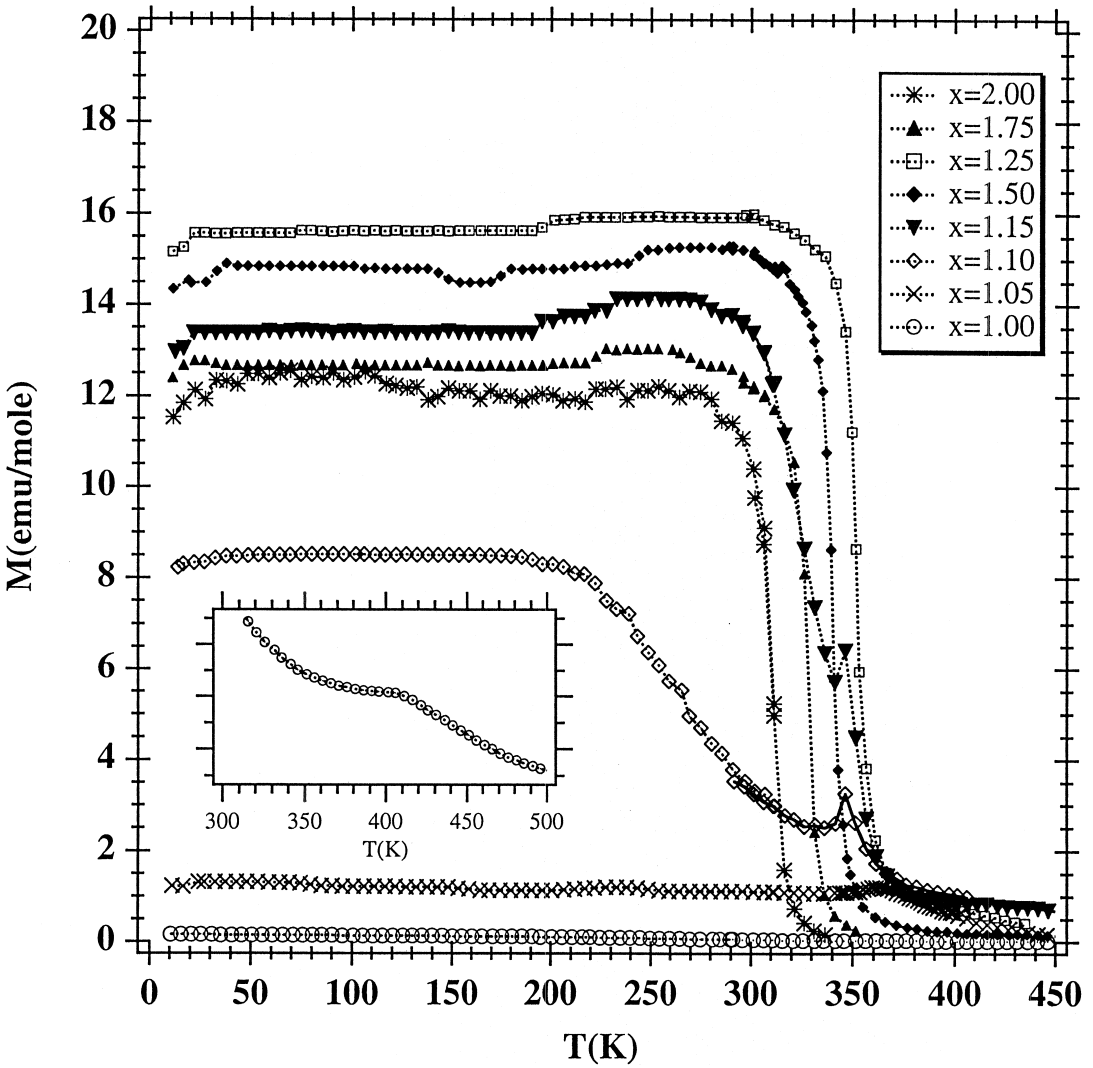

Fig. 5. Temperature dependence of the magnetization of $YMn_6Ge_{6-x}Ga_x$ ($1.0 \leq x \leq 2.0$) in an applied field of 0.025 T (insert shows the Néel point of the $YMn_6Ge_5Ga_1$ compound).

the general behaviour of the MMn_6X_6 compounds may be fairly well depicted considering a strong intraplane J_0 interaction, two short range interplane ferromagnetic J_1 and J_2 interactions and a long range interplane antiferromagnetic J_3 interaction mediated by the conduction electrons. The J_2 interaction is weaker than the J_1 interaction (due to different occupations of the Mn–X–Mn and Mn–(X,R)–Mn sheets) and is weak enough to compete with the long range J_3 interaction.

Owing to this scheme, the properties of the $YMn_6Ge_{6-x}Ga_x$ solid solution may be interpreted on the basis of x dependent J_2 and J_3 relative strengths. The transition from anti- to ferromagnetism should be related either to an enhancement of the positive J_2 interaction or to a weakening of the negative J_3 interaction. The strong lowering of the ordering temperatures in the antiferromagnetic state suggests a weakening of the J_3 interaction. In such a case, the decrease of this long range interaction mediated by the conduction electrons may be related to different DOS at the Fermi level.

Such an evolution of the magnetic interactions and the transitions observed by magnetization measurements allow a prediction of the x–T magnetic phase diagram of the $YMn_6Ge_{6-x}Ga_x$ system. The low gallium content compounds ($x \leq 0.25$) should remain antiferromagnetic. The low-temperature transitions observed in the $x = 0.5$ and 0.75 compounds may be related to an antiferromagnetic-to-helimagnetic transition. The $x = 1.0$ and 1.05 compounds might be characterized by helimagnetic structures in the whole ordering range, while the $x = 1.1$ and 1.15 compounds should display helimagnetic-to-ferromagnetic transitions. Finally, ferromagnetic structures should prevail for relatively high gallium contents ($x \geq 1.25$). It is worth noting that the thermal variation of the threshold fields indicates a decrease of the antiferromagnetic interactions with temperature. This behaviour is quite different to that

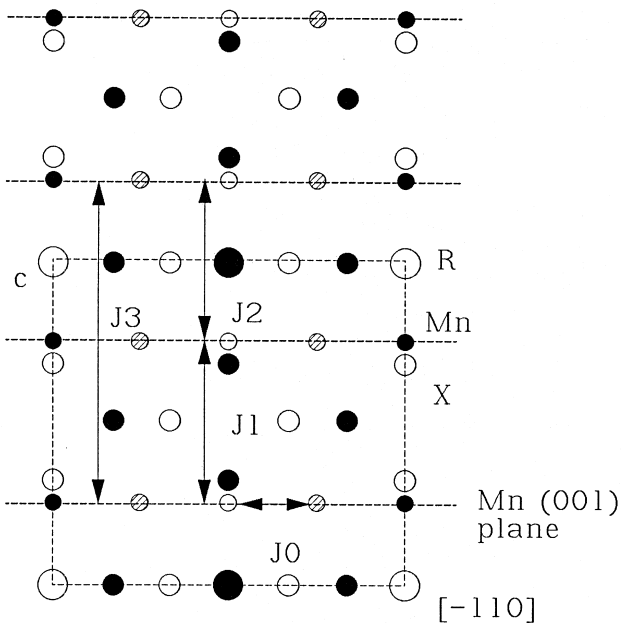

Fig. 6. Projection along [110] of the RMn_6X_6 structure showing the main Mn–Mn interactions.

observed in $SmMn_2Ge_2$, for instance [21], where antiferromagnetic interactions prevail at low temperature.

5. Conclusions

The results of the $YMn_6Ge_{6-x}Ga_x$ magnetic study open a wide field for further investigations.

It will now be interesting to complete this study by neutron diffraction experiments on selected compounds in order to determine precisely the x–T magnetic phase of this system. High-field magnetization measurements should provide interesting information on the evolution of the threshold fields as a function of the Ga content.

A magnetic study of $LuMn_6Ge_{6-x}Ga_x$ and $ScMn_6Ge_{6-x}Ga_x$ should provide additional information on the interplay between the interatomic spacings and the magnetic interactions. The low-temperature helimagnetic structure of $ScMn_6Ge_6$ suggests weaker antiferromagnetic interactions in this compound. With such an assumption, it is expected that smaller Ga contents should induce ferromagnetism.

It will also be interesting to check the magnetic properties of IVA solid solutions such as $ZrMn_6Ge_{6-x}Ga_x$ or $HfMn_6Ge_{6-x}Ga_x$. Such a study should provide some information on the interplay between valence electron concentration and Mn–Mn magnetic interactions.

The properties of the helimagnetic RMn_6Sn_6 (R = Sc, Y, Lu) compounds suggests weaker antiferromagnetic interactions. Moreover, the thermal variation of the propagating vectors indicates that the antiferromagnetic character decreases with temperature. Therefore, it may be assumed that replacement of tin by gallium or indium should rapidly induce ferromagnetism in these compounds. Owing to the thermal variation of the propagating vector, low-temperature helimagnetic-to-ferromagnetic transitions are also expected.

The results of the present experiments seems to indicate that the substitution of Ga for Ge enables a tuning of the Mn–Mn magnetic interactions. This property may provide new information on the interplay of the Mn–R couplings by studying paramagnetic R solid solutions. It will be particularly interesting to undertake a neutron diffraction study on helimagnetic $RMn_6Ge_{6-x}Ga_x$ compounds and to check the evolution of the Mn moment angles in the Mn–X–Mn sheet. If Ga substitution mainly reduces the strength of the J_3 interaction, it is expected that the J_1–J_3 competition will be weaker and that the turning angle will be smaller.

Due to the interplay between the magnetic exchange and the magneto-crystalline anisotropy of both sublattices, the magnetic structures of paramagnetic RMn_6Ge_6 compounds are rather complicated [17–20]. The stabilization of collinear ferrimagnetic structures by substitution of other elements for Ge should provide interesting information on the role of the magneto-crystalline anisotropy alone.

References

[1] G. Venturini, B. Chafik El Idrissi, B. Malaman, J. Magn. Magn. Mater. 94 (1991) 35.
[2] G. Venturini, R. Welter, B. Malaman, J. Alloys Comp. 185 (1992) 99.
[3] J.H.V.J. Brabers, V.H.M. Duijn, F.R. de Boer, K.H.J. Buschow, J. Alloys Comp. 198 (1993) 127.
[4] D.M. Clatterbuck, K.A. Gschneidner Jr., J. Magn. Magn. Mater. 207 (1999) 78.
[5] G. Venturini, R. Welter, B. Malaman, E. Ressouche, J. Alloys Comp. 200 (1993) 51.
[6] P. Schobinger-Papamantellos, G. André, J. Rodriguez-Carvajal, J.H.V.J. Brabers, K.H.J. Buschow, J. Alloys Comp. 226 (1995) 152.
[7] G. Venturini, D. Fruchart, B. Malaman, J. Alloys Comp. 236 (1996) 102.
[8] T. Mazet, R. Welter, G. Venturini, E. Ressouche, B. Malaman, Solid State Commun. 110 (1999) 407.
[9] T. Mazet, G. Venturini, R. Welter, B. Malaman, J. Alloys Comp. 264 (1998) 71.
[10] T. Mazet, R. Welter, B. Malaman, J. Alloys Comp. 284 (1999) 54.
[11] G. Venturini, A. Vernière, J. Alloys Comp. 298 (2000) 213.
[12] J.H.V.J. Brabers, Q.A. Li, F.R. deBoer, K.H.J. Buschow, IEE Trans. Magn. 30 (2) (1994) 1190.
[13] B. Chafik El Idrissi, B. Malaman, D. Fruchart, J. Less-Common Met. 175 (1991) 143.
[14] B. Malaman, G. Venturini, R. Welter, J.P. Sanchez, P. Vuillet, E. Ressouche, J. Magn. Magn. Mater. 202 (1999) 519.
[15] G. Venturini, B. Chafik El Idrissi, E. Ressouche, B. Malaman, J. Alloys Comp. 216 (1994) 243.
[16] P. Schobinger-Papamantellos, J. Rodriguez-Carvajal, G. André, K.H.J. Buschow, J. Magn. Magn. Mater. 150 (1995) 311.

[17] P. Schobinger-Papamantellos, F.B. Altofer, J.H.V.J. Brabers, F.R. de Boer, K.H.J. Buschow, J. Alloys Comp. 203 (1994) 243.
[18] P. Schobinger-Papamantellos, J.H.V.J. Brabers, K.H.J. Buschow, J. Magn. Magn. Mater. 139 (1995) 119.
[19] P. Schobinger-Papamantellos, G. André, J. Rodriguez-Carvajal, K.H.J. Buschow, J. Alloys Comp. 219 (1995) 176.
[20] P. Schobinger-Papamantellos, G. André, J. Rodriguez-Carvajal, J.H.V.J. Brabers, K.H.J. Buschow, J. Alloys Comp. 226 (1995) 113.
[21] E.M. Gyorgy, B. Batlogg, J.P. Remeika, R.B. van Dover, R.M. Fleming, H.E. Bair, G.P. Espinosa, A.S. Cooper, R.G. Maines, J. Appl. Phys. 61 (1987) 4237.